C Journal of Carbon Research

MDPI

Article

Rice Husk-Derived High Surface Area Nanoporous Carbon Materials with Excellent Iodine and Methylene Blue Adsorption Properties

Lok Kumar Shrestha [1,*], Mamata Thapa [2], Rekha Goswami Shrestha [1], Subrata Maji [1], Raja Ram Pradhananga [2] and Katsuhiko Ariga [1,3]

1 International Center for Materials Nanoarchitectonics (WPI-MANA), National Institute for Materials Science (NIMS), 1-1 Namiki, Ibaraki Tsukuba 305-0044, Japan; rekhashrestha3@hotmail.com (R.G.S.); MAJI.Subrata@nims.go.jp (S.M.); ARIGA.Katsuhiko@nims.go.jp (K.A.)

2 Amrit Science Campus, Tribhuvan University, Kathmandu 44613, Nepal; thapamamata2424@gmail.com (M.T.); rajaram2620@gmail.com (R.R.P.)

3 Graduate School of Frontier Sciences, The University of Tokyo, Kashiwa, Chiba 277-0827, Japan

* Correspondence: SHRESTHA.Lokkumar@nims.go.jp; Tel.: +81-29-860-4809

Received: 26 January 2019; Accepted: 19 February 2019; Published: 22 February 2019

Abstract: Iodine and methylene blue adsorption properties of the high surface area nanoporous carbon materials derived from agro-waste and rice husk is reported. Rice husk was pre-carbonized at 300 °C in air followed by leaching out the silica nanoparticles by extraction with sodium hydroxide solution. The silica-free rice husk char was mixed with chemical activating agents sodium hydroxide (NaOH), zinc chloride ($ZnCl_2$), and potassium hydroxide (KOH) separately at a mixing ratio of 1:1 (wt%) and carbonized at 900 °C under a constant flow of nitrogen. The prepared carbon materials were characterized by scanning electron microscopy (SEM), Fourier transformed-infrared spectroscopy (FT-IR), powder X-ray diffraction (pXRD), and Raman scattering. Due to the presence of bimodal micro- and mesopore structures, KOH activated samples showed high specific surface area ca. 2342 m^2/g and large pore volume ca. 2.94 cm^3/g. Oxygenated surface functional groups (hydroxyl, carbonyl, and carboxyl) were commonly observed in all of the samples and were essentially non-crystalline porous particle size of different sizes (<200 μm). Adsorption study revealed that KOH activated samples could be excellent material for the iodine and methylene blue adsorption from aqueous phase. Iodine and methylene blue number were ca. 1726 mg/g and 608 mg/g, respectively. The observed excellent iodine and methylene blue adsorption properties can be attributed to the well-developed micro- and mesopore structure in the carbon material. This study demonstrates that the agricultural waste, rice husk, and derived nanoporous carbon materials would be excellent adsorbent materials in water purifications.

Keywords: rice husk; nanoporous carbon materials; chemical activation; iodine adsorption; methylene blue adsorption

1. Introduction

Activated nanoporous carbons materials (NCMs) represent porous carbonaceous materials that have been processed to increase porosity and specific surface area so that they can be widely used as adsorbents to adsorb metal ions and organic molecules, catalysts, and catalyst supports for the removal of pollutant species from gases or liquids and as electrode materials for batteries and supercapacitors [1–6]. Depending on the synthetic method, conditions, and precursor type, NCMs with tunable porosity, surface area, and surface functionality can be prepared [6–8]. Generally, surface area and pore volume of porous carbon materials range from 250–2410 m^2/g and 0.022–91.4

cm^3/g, respectively [9]. Direct carbonization and activation of the carbonaceous precursors are the general methods for the fabrication of NCMs. Direct carbonization is performed by mild- or high temperature heat-treatment in which pyrolytic decomposition of the precursor occurs with the elimination of many non-carbon elemental species (H, N, O and S), resulting in the formation of fixed carbonaceous char with porous structure. On the other hand, activation processes can be either physical or chemical [10–12]. Physical activation includes two-step processes involving carbonization of the precursor material, followed by gasification of the char at elevated temperatures between 800 to 1100 °C using oxidants such as steam, carbon dioxide, air, or the mixture of these gases [13]. On the other hand, chemical activation is a single step process, which is usually carried out by mixing precursor material or pre-carbonized char with chemical activating agents (acids, alkali, or salts) and carbonize at moderate temperature ranges between 400 to 800 °C under the inert gas atmosphere of nitrogen or argon [14,15]. Nevertheless, sometimes chemical activation was performed in harsh conditions at higher temperatures of up to 1000 °C [16]. Investigations have shown that the chemical activation method is advantageous over physical activation, as it operates at a lower temperature and the process is time saving. More to this, activating chemicals used during chemical activation act as the dehydrating agent, which inhibits the formation of tar and thus reduce the production of other volatile products. As a result, high yield carbon with very high surface area and well-developed porosity can be obtained [17–20].

NCMs have been used in various technological fields including sensing, separation, environmental safety, and energy storage. Investigations have shown that the performance of NCMs highly depends on the surface area, pore volume, and surface functional groups. Generally, the higher the surface area, the better the performance. Therefore, attention has been paid to the production of scalable high surface area nanoporous carbon materials, particularly in a cost effective way from agricultural by-products or wastes. Wide varieties of carbonaceous precursor materials including pitch [21], pistachio shell [22], rice husks [23,24], coconut shell [25], eucalyptus wood [26], firewood [27,28], oil-palm shell [29,30], babassu [31], corncob [32], bamboo [33,34], etc. have been used to prepare activated carbons. It is anticipated that successful production of high surface area and large pore volume NMCs from agro-wastes would contribute to address the current problems related to the environment and energy storage. Various agricultural wastes have been explored as potential carbon precursors [35,36]. The choice of precursor for the preparation of NCMs depends on the availability, cost, and carbon content in the precursor. Among various agricultural wastes, rice husk, which is undesirable agricultural mass residue and has posed disposal problems, could be an excellent low cost precursor for the production of activated carbon materials [37]. It has been reported that rice husks have a low calorific value of 3585 kcal kg^{-1} and high ash content of ~ 22%. Dry rice husk contains 70–85% organic matter (21.44% lignin, 32.24% cellulose, 21.34% hemicellulose) and inorganic remainder (20–25%) consists of silica [38,39]. Not limited to the porous carbon material, rice husk ash has also been used in synthesis of silica, silicon based materials, zeolite, catalysts, ingredients for lithium ion batteries, graphene, energy storage/capacitor, etc. [40–50]. Using both physical and chemical activation methods, activated carbons can be prepared from rice husks [51,52]. The silica embedded in rice husk as nanoparticles [53] can be leached out using chemical activating agents and thus the leaching out of the silica causes pore formation in the carbon material [54].

In this contribution, we report a novel yet simple method for the preparation of high surface area nanoporous activated carbon materials from rice husk, and their iodine and methylene blue adsorption properties. Despite the conventional method of direct carbonization or activation at a lower temperature, our method includes pre-carbonization of a precursor (rice husk) at 300 °C, chemical etching with NaOH for the removal of silica, and then chemical activation at a high temperature of 900 °C using NaOH, $ZnCl_2$, and KOH activating agents. NaOH-treated pre-carbonized rice husk char was mixed with an activating agent at a mixing ratio of 1:1 by weight and the effect of activating agents on surface area, surface morphology and iodine, and methylene blue adsorption properties were investigated. The prepared nanoporous carbon materials were well characterized by Fourier

transform-infrared (FT-IR) spectroscopy, Raman scattering, powder X-ray diffraction (XRD), and scanning electron microscopy (SEM). Surface textural properties including surface area and pore volume were determined by nitrogen adsorption/desorption measurements. The KOH activated optimal sample (with surface area ca. 2342 m^2/g and total pore volume ca. 2.94 cm^3/g) showed excellent iodine and methylene blue adsorption properties giving iodine and methylene blue numbers ca. 1726 and 608 mg/g, respectively. These values are much higher than observed in commercial activated carbon, demonstrating that nanoporous carbon materials derived from rice husk using this method would have potential in water purification.

2. Materials and Methods

2.1. Materials

The analytical grade chemicals potassium hydroxide (KOH), sodium hydroxide (NaOH), zinc chloride ($ZnCl_2$), potassium iodide (KI), hydrochloric acid (HCl), and sodium thiosulfate ($Na_2S_2O_3 \cdot 5H_2O$) were purchased from Qualigen (Mumbai, India). Analytical grade methylene blue was a product of Loba-Chemie, Mumbai, India. All the chemicals were used as received. Millipore filter water was used to prepare solutions.

2.2. Preparation of Nanoporous Carbon Material (NCM)

Rice husk was treated with 5% HCl, washed with distilled water several times, and dried in a hot air oven (Toshniwal, Ajmer, India) at 100 °C for 6 h. Dried rice husk was pyrolyzed in a muffle furnace (Vitco India, Sunvic in U.K.) at 300 °C for 3 h and the product was grinded into powder form in a grinder (Signoracare, Haryana, India) and sieved through a sieve of 250 microns mesh size. The obtained product is referred to as rice husk char (RHC). For leaching out the silica from the pyrolyzed product, RHC (200 mg) was mixed with NaOH solution (200 mL: 1 M) and heated for 30 min at 70 °C and cooled down to room temperature naturally and filtered out. After several washings with pure water, the residue was washed with HCl solution (0.1 M) and further with pure water until the filtrate gave a neutral litmus test. The residue was collected and dried in a hot air oven for 12 h at 80 °C and thus was prepared and referred to as RHC_NaOH. Rice husk char prepared after leaching out the silica (RHC_NaOH) was mixed with NaOH, $ZnCl_2$, and KOH separately in the mixing ratio of 1:1 by weight and stored for 24 h at 25 °C before carbonization. Carbonization was then performed at 900 °C in a tubular furnace (KOYO, Tokyo, Japan) under the continuous flow of nitrogen (120 cc/min) for 4 h. The carbonized samples were washed with HCl solution (0.1 M) and water until a neutral pH was achieved. The obtained products were then dried in a hot air oven at 80 °C for 24 h and referred to as NCM_N (NaOH activated), NCM_Z ($ZnCl_2$ activated), and NCM_K (KOH activated).

2.3. Characterizations

The prepared RHC, RHC_NaOH, and NCMs (NCM_N, NCM_Z and NCM_K) were characterized by powder X-ray diffraction (pXRD: Rigaku RINT2000 diffractometer, Rigaku, Tokyo, Japan with Cu-Kα radiation λ = 0.1541 nm), scanning electron microscopy (SEM) operated at 10 kV (SU-8000, Hitachi, Tokyo Japan), Raman scattering spectroscopy (T64000, Jobin-Yvon Edison, Edison, NJ, USA: at excitation wavelength of 514.5 nm), and Fourier transform infrared (FT-IR) spectroscopy (Nicolet 4700 instrument, Nicolet, Walthan, MA, USA). SEM samples were prepared by drop casting dilute suspensions of NCMs in IPA on a clean silicon wafer and dried at 80 °C for 6 h before SEM observations. SEM samples were coated with platinum (~ 2 nm) by sputtering using a Hitachi S-2030 ion coater (Tokyo, Japan). Electron dispersive X-ray spectroscopy (EDX) analyses were carried out on uncoated samples using a Horiba Model EMAX 7593-H (Kyoto, Japan) accessory interfaced with a Hitachi S-4800 SEM instrument. Surface area (Brunauer-Emmett-Teller (BET)) and pore volume were determined by recording N_2 adsorption-desorption isotherms on an automatic adsorption instrument (Quantachrome Instrument, Autosorb-1, Boynton Beach, FL, USA).

2.4. Iodine and Methylene Blue Adsorption

Iodine and methylene blue adsorption properties of the prepared NCMs were studied and the iodine numbers and methylene blue values were determined. The iodine numbers were determined according to the ASTM D4607-94 method (2006) [55]. This method is based on three points isotherm. NCMs (100 mg) was separately taken in a conical flask and HCl solution (5 mL: 5% v/v) was added and heated until the solution boiled and cooled down. Iodine solution (10 mL: 0.05 M) was then added. The mixtures were vigorously shaken for about 4 min and filtered out. The filtrate solution (10 mL) was titrated against standard hypo solution (0.1 M) using starch as an indicator. The iodine amount adsorbed per gram of carbon was calculated and was plotted against the iodine concentration in the filtrate. A least square fitting regression was applied for the three points. The iodine number is the value of iodine adsorbed per gram of activated carbon when residual concentration was 0.02 N. The amount of iodine adsorbed per gram of NCM was calculated as follows.

$$\text{Iodine adsorbed per gram of } NCM = C * \text{Conversion factor } (f) \tag{1}$$

The conversion factor (f) is defined as:

$$\text{Conversion factor } (f) = \frac{\text{Molecular weight} * \text{Normality of Iodine} * 10}{\text{Weight of carbon} * \text{Blak reading}} \tag{2}$$

C = (Blank reading $-$ volume of hypo consumed after adsorption of carbon material)

Methylene blue numbers of NCMs were determined with a multi-point isotherm adsorption using Langmuir model. NCMs (0.1 g) were mixed with methylene blue solution (100 mL) of different concentrations 25, 50, 100, 150, 200, 500, and 1000 mg/L in dry and clean conical flasks. Using a mechanical shaker, the mixture was shaken for 24 h, the suspensions were filtered out, and the remaining concentration was measured spectrophotometrically at λ_{max} of 660 nm using UV/VIS spectrophotometer (LT-2802 Labtronic, Haryana, India). The amount of methylene blue adsorbed was determined and methylene blue adsorbed per gram of NCM was calculated by using Equation (3) [56].

$$q_e(\text{mg/gm}) = \frac{(C_0 - C_e)V}{M} \tag{3}$$

where, q_e (mg/gm) = amount of methylene blue adsorbed; C_o (mg/L) = the initial concentration of methylene blue; C_e (mg/L) = the equilibrium concentration of methylene blue; V (L) = the volume of methylene blue and M (gm) = the mass of NCM taken.

To determine the methylene blue number linearized form Langmuir isotherm (Weber Equation (4)) was used in which q_e/c_e was plotted against c_e and by least square fitting regression the maximum amount of methylene blue adsorbed by 1 gram of NCM, qmax, the methylene blue number was calculated.

$$\frac{c_e}{q_e} = \frac{1}{b\, q_{max}} + \frac{c_e}{q_{max}} \tag{4}$$

3. Results and Discussion

Using FT-IR spectroscopy, surface functional groups in the prepared materials (RHC, RHC_NaOH, NCM_N, NCM_Z, and NCM_K) were studied. As anticipated, various surface functional groups are present in RHC and RHC_NaOH samples (Figure 1a). However, most of the functional groups disappeared in NCMs due to high temperature carbonization (Figure 1b).

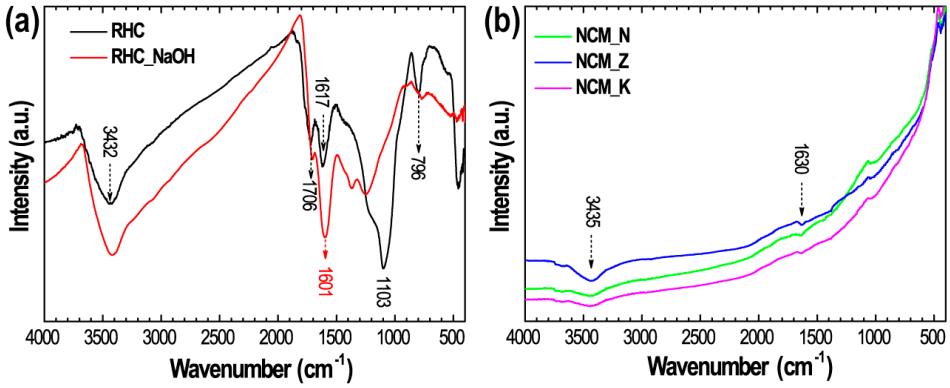

Figure 1. (**a**) FT-IR spectra of RHC and RHC_NaOH, and (**b**) FT-IR spectra of NCM_N, NCM_Z, and NCM_K recorded at 25 °C.

FT-IR spectra indicates that the surface functional groups of the NCMs derived from rice husk using different activating agents do not exhibit significant differences. All the NCMs exhibit hydroxyl and carbonyl functional groups (Figure 1b). In the FT-IR spectra, broad band in the range of 3200 to 3600 cm^{-1} (approximately centered at 3430 cm^{-1}) can be assigned to stretching vibration of O–H bonds corresponding to alcohol, phenol, or adsorbed moisture [56]. Peak around 1700 cm^{-1} refers to the stretching vibrations of C=O bond of carboxylic group and the peak around 1600 cm^{-1} can be attributed to C=C stretching vibration in the aromatic ring. Peak at 1100 cm^{-1} to 1200 cm^{-1} refers to the stretching of C–O bonds and the peak around 800 cm^{-1} is due to the stretching vibration of Si–O bond [57,58]. RHC as obtained by heating in air at 300 °C exhibits Si–O bond, which after washing with NaOH solution, disappeared in RHC_NaOH sample, indicating the removal of silica embedded in the RHC. Removal of silica is further confirmed by SEM/EDX. Figure 2 shows SEM/EDX elemental mapping results for RHC and RHC_NaOH. Absence of Si in the elemental mapping of the RHC_NaOH (Figure 2h) confirms the removal of silica.

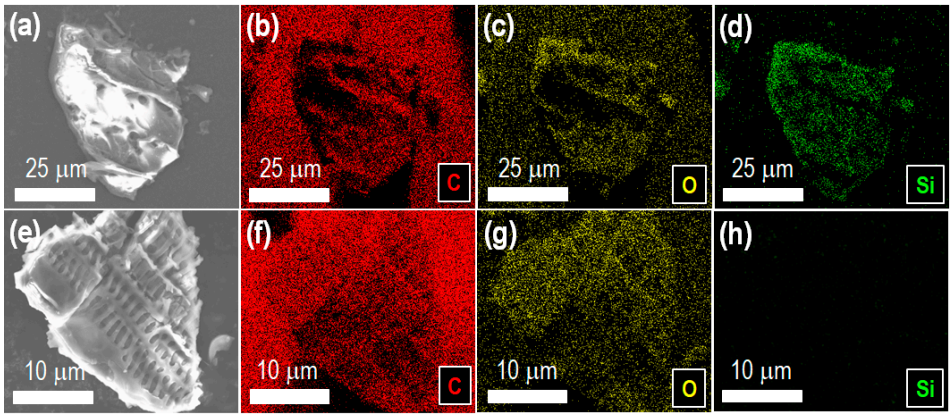

Figure 2. Results obtained from SEM/EDX. (**a**) SEM image of RHC, and elemental mapping (**b**) carbon, (**c**) oxygen and (**d**) silicon, and (**e**) SEM image of RHC_NaOH, and elemental mapping (**f**) carbon, (**g**) oxygen, and (**h**) silicon.

Using scanning electron microscopy, surface morphology, and structure of the prepared RHC, NaOH treated RHC and the derived NCMs were studied. Fine granules with a size <200 microns and containing many macropores on the surface can be seen in all the samples. Figure 3 shows the typical SEM images at different magnifications showing macro and mesopores. RHC obtained after pyrolysis of rice husk does not contain micro/mesopores (Figure 3a–c). This is because of the silica embedded in the carbon. However, when RCH was treated with NaOH, silica dissolves forming soluble sodium silicate, which was washed out with water and pores were generated. Honey-comb

like macroporous structures can be seen in the RHC_NaOH sample (Figure 3d,e). However, merely NaOH treatment did not lead to the formation of micro- or mesopores (Figure 3f). We have also studied the effect of NaOH treatment reaction time on the surface porous structure, extending reaction time up to 1 h. However, we did not observe substantial differences on the porosity. Uniform macroporous structure may be expected at extended reaction times (say 6 h or 12 h), but its contribution to the surface textural properties (surface area and pore volume) will be minimal because of a lack of micro- and mesoporous structure. Development of mesoporous structure can be seen after NaOH, $ZnCl_2$, and KOH chemical activation at 900 °C (Figure 3g–o). Porosity seems smaller in the NaOH activated sample, NCM_N (Figure 3i) compared to the $ZnCl_2$ (NCM_Z) and KOH (NCM_K) activated samples (Figure 3l,o) demonstrating that $ZnCl_2$ and KOH are the better activating agents for the development of micro/mesopore structure in the carbon.

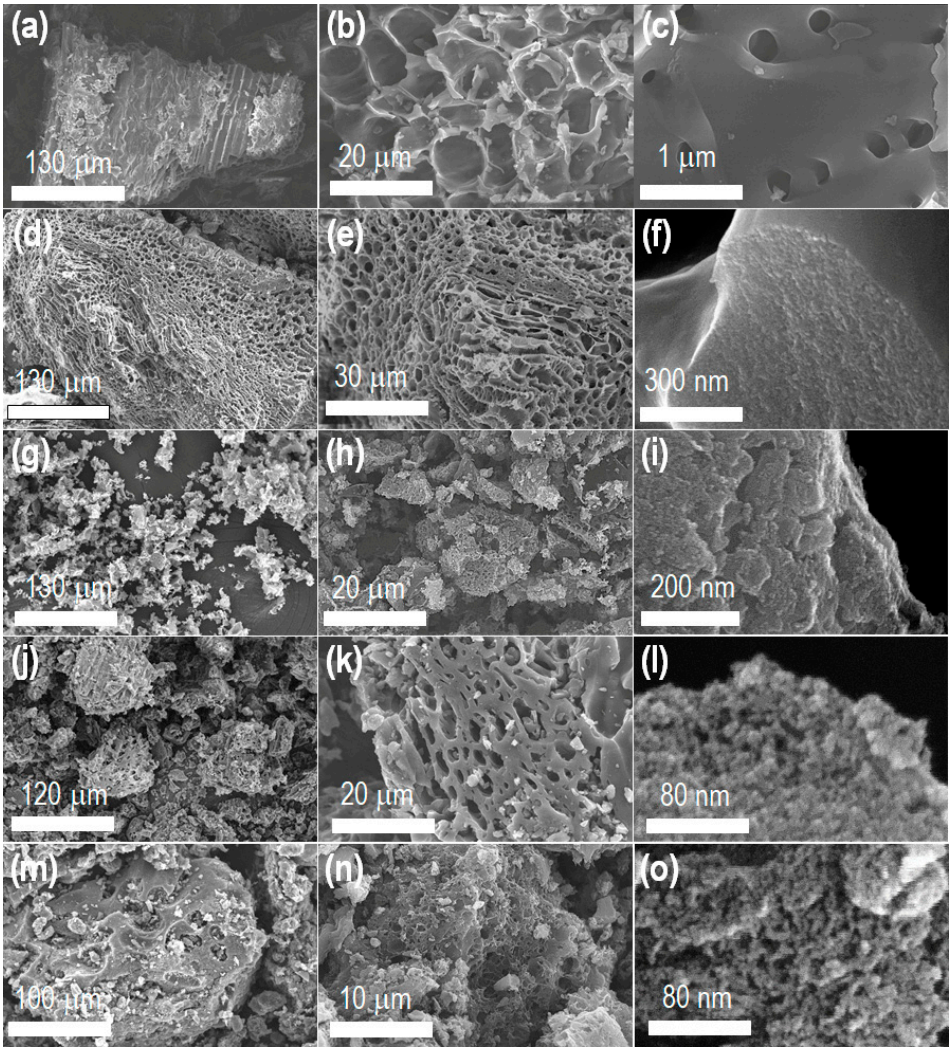

Figure 3. SEM images of the prepared materials as typical example. (**a**–**c**) RHC, (**d**–**f**) RHC_NaOH, (**g**–**i**) NCM_N, (**j**–**l**) NCM_Z, and (**m**–**o**) NCM_K.

Powder X-ray diffraction patterns showed amorphous carbon structure. Two broad pXRD peaks (Figure 4a) observed for the NCM_Z and NCM_K samples at diffraction angles, 2θ ~25 and 43 degree represent typical features of amorphous carbons. These peaks corresponded to the (002) and (101) planes of micrographitic clusters formed during activation process at elevated temperatures [59–61]. Due to low processing temperature, in RHC and RHC_NaOH samples, ordered graphitic layers were not fully developed, and as a result pXRD peaks corresponding to (101) plane are absent. On the

other hand, a sharp diffraction peak appeared at 2θ ~26 degrees for the NCM_N sample indicated the formation of highly graphitic carbon clusters, which is in agreement with the previous report that NaOH activation at high temperature leads to perfection in the crystalline graphitic structure [62].

Using the Raman scattering technique, the graphitization degree, defects, and bonding states of the prepared nanoporous carbon material were studied [63]. As seen in Figure 4b, Raman scattering spectra of all the samples exhibit two broad bands at 1345 (D) and 1590 cm^{-1} (G), corresponding to the typical amorphous carbons [64]. The defect induced D band in the Raman spectrum represents the disordered carbon structure and corresponds to sp^3 carbon, while the graphitic G band is coming from the E_{2g} mode and arises from C–C bond stretching in graphitic carbon materials [60,65]. The G band is commonly observed in all sp^2 carbon systems such as carbon nanotubes, graphene, and fullerenes. The relative intensity of the G and D bands (I_G/I_D), which measures the degree of graphitization, is exceptionally high in NCM_N (I_G/I_D ca. 1.23), which indicates the fact that NaOH activation caused higher degree of graphitization. The rest of the samples have essentially the same degree of graphitization I_G/I_D ca. in the range of 1.01 to 1.16, which is similar to that observed in commercial active carbons.

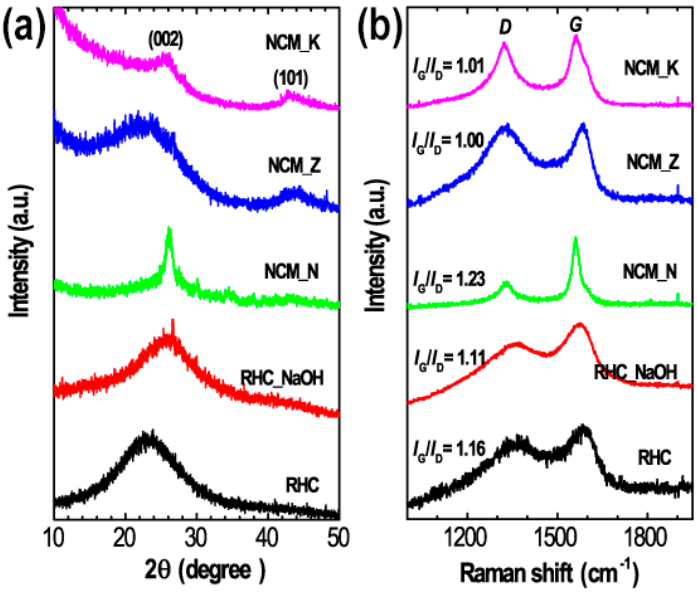

Figure 4. (**a**) pXRD patterns, and (**b**) Raman scattering spectra of RHC, RHC_NaOH, NCM_N, NCM_Z, and NCM_K recorded at 25 °C.

Figure 5 shows nitrogen adsorption-desorption isotherms, and the pore size distributions obtained by Barrett-Joyner-Halenda (BJH) and density functional theory (DFT). As it can be seen, nitrogen sorption isotherm is very much different depending on the sample indicating that the activating agent plays an important role on the surface area and pore volume of the prepared NCMs. Nitrogen adsorption capacity of RHC and RHC_NaOH before chemical activation is very low, which indicates the low porosity development in these sample as revealed by SEM observation. However, after chemical activation, nitrogen adsorption of the rice husk derived NCMs is enhanced drastically and the materials displayed mixed Type-I/Type-IV adsorption isotherms [64,66]. Significant increase of nitrogen adsorption at lower relative pressure with a hysteresis loop at higher relative pressures (Figure 5a: NCM_K) is a typical sorption isotherm of porous materials containing both micro- and mesopore structures. High nitrogen adsorption at lower relative pressure is well-known phenomena of micropore filling, whereas capillary condensation occurring in the mesopores is responsible for the hysteresis loop. The pore size distribution curves shown in Figure 5b (BJH method) and Figure 5c (DFT method) further confirm the presence of meso- and microporous structure of the NCMs. From the adsorption isotherms Brunauer-Emmett-Teller (BET), surface areas were ca. 885 m^2/g (NCM_N),

1264 m^2/g (NCM_Z), and 2342 m^2/g (NCM_K). The BET surface areas of pre-carbonized samples before activation were very poor and were ca. 156 m^2/g (RHC) and 214 m^2/g (RHC_NaOH). Similarly, total pore volumes of the prepared NCMs were ca. 1.18 cm^3/g (NCM_N), 1.99 cm^3/g (NCM_Z) and 2.94 cm^3/g (NCM_K), while that of non-activated samples were ca. 0.26 cm^3/g (RHC) and 0.46 cm^3/g (RHC_NaOH). The average pore size of chemically activated NCMs were ca. 5.37 nm (NCM_N), 3.26 nm (NCM_Z) and 5.0 nm (NCM_K). It is interesting to note that KOH activated sample displayed excellent surface textural properties BET surface area (2342 m^2/g), which is much higher than most of the commercially available activated carbons, whose surface area were found in the range of 1000–1200 m^2/g [64,67].

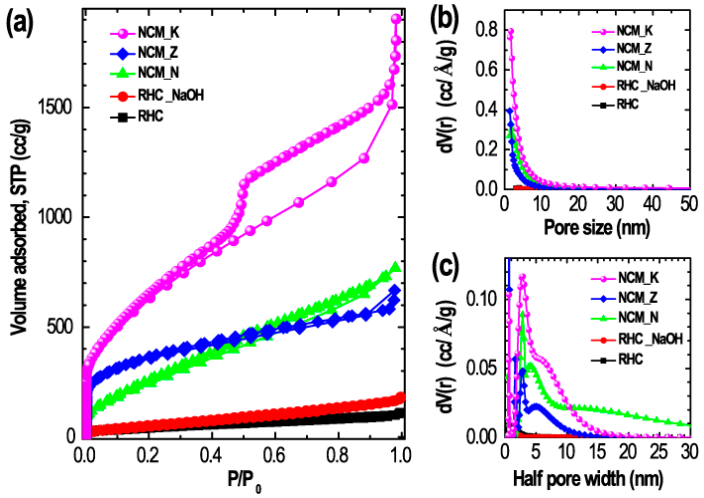

Figure 5. (**a**) Nitrogen adsorption-desorption isotherms of RHC, RHC_NaOH, NCM_N, NCM_Z, and NCM_K, (**b**) Corresponding pore size distribution curves as obtained from BJH method, and (**c**) Corresponding pore size distribution curves as obtained from DFT method.

Table 1 compares the surface textural properties (surface area and pore volume) of our NCMs with similar nanoporous carbon materials derived from other agricultural wastes [35].

Table 1. Comparison of surface area and pore volume of our NCMs (derived from rice husk) with similar nanoporous carbon materials derived from other agro wastes by chemical activation method with different activating agents.

Precursors	Activating Agents	Temperature (°C)	BET Surface Area (m^2/g)	Pore Volume (cc/g)
Sugarcane baggage	$ZnCl_2$	400	736	0.34
Corn cob	$ZnCl_2$	400	1370	0.62
Corn cob	H_3PO_4	400	1288	1.64
Bamboo	$ZnCl_2$	400	1435	0.63
Bamboo	H_3PO_4	400	1431	1.10
Bamboo	H_3PO_4	500	1340	2.01
Bamboo	H_3PO_4	600	2129	2.69
Lapsi seed	$ZnCl_2$	400	1233	0.55
Lapsi seed	NaOH	400	1002	0.26
Rice husk (this work)	NaOH	900	885	1.18
Rice husk (this work)	$ZnCl_2$	900	1264	1.99
Rice husk (this work)	KOH	900	2342	2.94

Inspired by the excellent surface area and pore volume of the rice husk derived nanoporous carbon material, we have investigated their iodine and methylene blue adsorption properties and iodine and methylene blue numbers were determined. The obtained results are also compared with commercial activated carbon and also RHC and RHC_NaOH before activation. Extensive investigations have been carried out on the adsorptive capacity of methylene blue on different adsorbents. Methylene blue number is an indication of adsorption capacity for large molecules

comparable to methylene blue. Raposo et al. [68] used a simple but very effective technique to evaluate the adsorption capacity of activated carbons and found that the adsorption process depends on several parameters, including pH, adsorbent concentration of adsorbate, contact time, and temperature. However, determination methylene blue number following the ASTM D 4507-97 method [55] is rather quick and gives quantitative information related to the adsorption capacity of activated carbon without going through rigorous study of kinetics of adsorption and fitting the experimental data into various models of adsorption isotherms. In the present investigation batch, adsorption tests were carried out at the original pH of the solution without any pH adjustment at 25 °C and varying the concentration of methylene blue from 25 to 1000 mg/L. The contact time of 24 hours was used to measure the isotherm of all samples. To determine the methylene blue number, a linearized form Langmuir isotherm (Equation (4)) was used in which q_e/c_e was plotted against c_e and by least square fitting regression the maximum amount of methylene blue adsorbed by 1 gram of NCM, q_{max}, (methylene blue number) was evaluated. The value of determination coefficients, R^2, was higher than 0.95.

Iodine number is a simple and quick method to evaluate the internal surface area of the carbon [69]. We have found that the iodine number of the materials ranges from 228 to 1726 mg/g, with the highest number for the RHC_K sample (1726 mg/g), which is more than double the commercial activated carbon (787 mg/g) (Figure 6a). Whereas the iodine number of l NCM_N (711 mg/g) and NCM_Z (863 mg/g) is comparable to that of the commercial activated carbon. As expected, due to a lack of well-developed porosity, an iodine number of RHC (228 mg/g) and RHC_NaOH (254 mg/g) is very low. It should be noted that the performance of NCMs is generally expressed through an iodine number. The higher the iodine number, the better the activation. Furthermore, the iodine number also measures the micro porosity of the NCMs. The observed the highest iodine number of the KOH activated NCM_K, therefore, indicates the well-developed micro porosity in the carbon material (as supported by the BET data) and this material would have potential in iodine adsorption or separation of iodine from aqueous phase.

Figure 6b shows the methylene blue (MB) numbers of the RHC, RHC_NaOH, NCM_N, NCM_Z, and NCM_K. The MB number ranges from 80 to 608 mg/g, again giving the maximum value for RHC_K sample (608 mg/g), which is exactly double the MB value obtained for commercial activated carbon (304 mg/g). The MB values for RHC_NaOH, NCM_N, and NCM_Z are comparable while that of RHC is extremely low (80 mg/g). The excellent methylene blue adsorption performance of our material demonstrate that rice husk derived high surface area nanoporous carbons would have potential in water purification for the removal of water soluble organic dyes form waste water or industrial effluents [67,70].

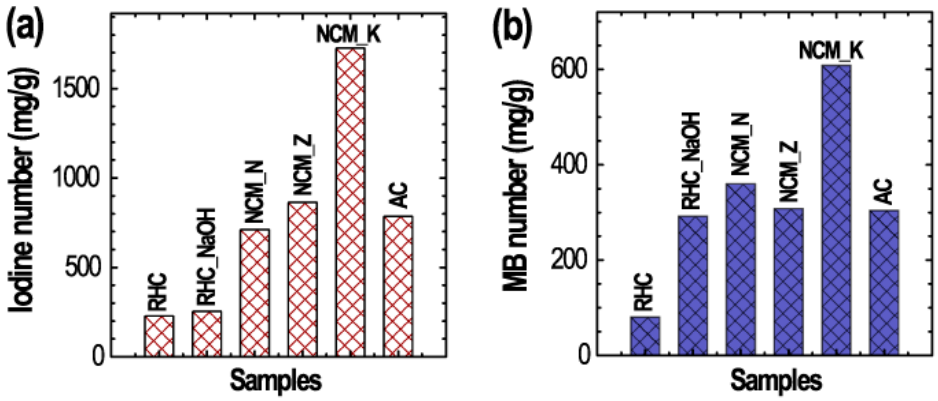

Figure 6. Results obtained from iodine and methylene blue adsorption: (**a**) Iodine numbers of RHC, RHC_NaOH, NCM_N, NCM_Z, and NCM_K, and (**b**) Corresponding methylene blue (MB) values.

4. Conclusions

Using agricultural waste and rice husk, we have fabricated high surface area nanoporous carbon material (2342 m^2/g) by modified physical/chemical activation method, which perform excellently for iodine and methylene blue adsorption giving iodine and methylene blue number of 1726 mg/g and 608 mg/g, respectively. The adsorption properties of our material is far better than the commercial activated carbon, demonstrating that the rice husk derived nanoporous carbon material would have potential as a high efficiency adsorbent in water purification. Since the starting material is low-cost agro-waste, scalable production of high surface area nanoporous carbon material would be an asset to sustainable technology.

Author Contributions: R.R.P. and L.K.S. conceived and designed the experiments; M.T., R.G.S., and S.M. performed the experiments; R.G.S., S.M., and R.R.P. analyzed the data; K.A. and L.K.S. contributed reagents/materials/analysis tools; L.K.S., and K.A. discussed the data and wrote the paper.

Funding: This research was partially funded by JSPS KAKENHI Grant Number JP 16H06518 (Coordination Asymmetry) and CREST JST Grant Number JPMJCR1665.

Acknowledgments: Mamata Thapa thanks the International Center for Materials Nanoarchitectonics (WPI-MANA) and National Institute for Materials Science (NIMS) for the internship award (Nov. 1, 2016 to Jan. 28, 2017).

Conflicts of Interest: The authors declare no conflict of interest.

References

1. Aboua, K.N.; Yobeuet, Y.A.; Yao, K.B.; Goné, D.L.; Trokourey, A. Investigation of dye adsorption onto activated carbon from the shells of Macoré fruit. *J. Environ. Manag.* **2015**, *156*, 10–14. [CrossRef] [PubMed]
2. Niu, B.; Lu, F.; Zhang, H.-Y.; Zhang, Y.; Zhao, J. Synthesis of nitriles from aerobic oxidation of amines catalyzed by ruthenium supported on activated carbon. *Bull. Chem. Soc. Jpn.* **2017**, *46*, 330–333. [CrossRef]
3. Mohan, E.H.; Anandan, S.; Rao, B.V.A.; Rao, T.N. Neem leaf-derived micro and mesoporous carbon as an efficient polysulfide inhibitor for sulful cathode in a Li-S battery. *Bull. Chem. Soc. Jpn.* **2019**, *48*, 62–64.
4. Li, B.; Zhang, H.; Wang, D.; Lv, H.; Zhang, C. Agricultural waste-derived activated carbon for high performance lithium-ion capacitors. *RSC Adv.* **2017**, *7*, 37923–37928. [CrossRef]
5. Shu, Y.; Dobashi, A.; Li, C.; Shen, Y.; Uyama, H. Hierarchical porous carbon from greening plant shell for electric double-layer capacitor application. *Bull. Chem. Soc. Jpn.* **2017**, *90*, 44–51. [CrossRef]
6. Shu, Y.; Maruyama, J.; Iwasaki, S.; Shen, Y.; Uyama, H. Activated carbon monolith derived from *Amygdalus pedunculata* shell and polyacrylonitrile for supercapacitors. *Bull. Chem. Soc. Jpn.* **2017**, *90*, 1333–1336. [CrossRef]
7. Khan, J.H.; Marpaung, F.; Young, C.; Lin, J.; Islam, M.T.; Alsheri, S.M.; Ahamad, T.; Alhokbany, N.; Ariga, K.; Shrestha, L.K.; et al. Jute-derived microporous/mesoporous carbon with ultra-high surface area using a chemical activation process. *Microporous Mesoporous Mater.* **2019**, *274*, 251–256. [CrossRef]
8. Khan, J.H.; Lin, J.; Young, C.; Matsagar, B.M.; Wu, K.C.-W.; Dhepe, P.L.; Islam, M.T.; Rahman, M.M.; Shrestha, L.K.; Alshehri, S.M.; et al. High surface area nanoporous carbon derived from high quality jute from Bangladesh. *Meter. Chem. Phys.* **2018**, *216*, 491–495. [CrossRef]
9. Ioannidou, O.; Zabaniotou, A. Agricultural residues as precursors for activated carbon production. *Renew. Sustain. Energy Rev.* **2007**, *11*, 1966–2005. [CrossRef]
10. Dolas, H.; Sahin, O.; Saka, C.; Demir, H. A new method on producing high surface area activated carbon: The effect of salt on the surface area and the pore size distribution of activated carbon prepared from pistachio shell. *Chem. Eng. J.* **2011**, *166*, 191–197. [CrossRef]
11. Joshi, S.; Shrestha, L.K.; Kamachi, Y.; Malgras, V.; Pradhananga, M.A.; Pokharel, B.P.; Naata, T.; Pradhananga, R.R.; Ariga, K.; Yamauchi, Y. Synthesis and characterizations of nanoporous carbon derived from Lapsi (*Choerospondias axillaris*) seed: Effect of carbonization conditions. *Adv. Powder Technol.* **2015**, *26*, 894–900. [CrossRef]
12. Joshi, S.; Shrestha, L.K.; Kamachi, Y.; Yamauchi, Y.; Pradhananga, M.A.; Pokhrel, B.P.; Ariga, K.; Pradhananga, R.R. Sodium hydroxide activated nanoporous carbons based on Lapsi seed stone. *J. Nanosci. Nanotechnol.* **2015**, *15*, 1465–1472. [CrossRef] [PubMed]

13. González, J.F.; Román, S.; González-García, C.M.; Nabais, J.M.V.; Ortiz, A.L. Porosity development in activated carbons prepared from walnut shells by carbon dioxide or steam activation. *Ind. Eng. Chem. Res.* **2009**, *48*, 7474–7481. [CrossRef]
14. Shrestha, L.K.; Shrestha, R.G.; Joshi, S.; Rajbhandari, R.; Shrestha, N.; Adhikari, M.P.; Pradhananga, R.R.; Ariga, K. Nanoarchitectonics of nanoporous carbon materials from natural resource for supercapacitor application. *J. Inorg. Organomet. Polym.* **2017**, *27*, S48–S56. [CrossRef]
15. Somasundaram, S.; Sekar, K.; Gupta, V.K.; Ganesan, S. Synthesis and characterization of mesoporous activated carbon from rice husk for adsorption of glycine from alcohol-aqueous mixture. *J. Mol. Liq.* **2013**, *11*, 416–425. [CrossRef]
16. Bedia, J.; Peñas-Garzón, M.; Gómez-Avilés, A.; Rodriguez, J.J.; Belver, C. A review on synthesis and characterization of biomas-derived carbons for adsorption of emerging contaminants from water. *C* **2018**, *4*, 63.
17. Ma, F.; Ding, S.; Ren, H.; Liu, Y. Sakura-based activated carbon preparation and its performance in supercapacitor applications. *RSC Adv.* **2019**, *9*, 2474–2483. [CrossRef]
18. Bergna, D.; Varila, T.; Romar, H.; Lassi, U. Comparison of the properties of activated carbons produced in one-stage and two-stage processes. *C* **2018**, *4*, 41. [CrossRef]
19. Han, J.; Kwon, J.H.; Lee, J.-W.; Lee, J.H.; Roh, K.C. An effective approach to preparing partially graphitic activated carbon derived from structurally separated pitch pine biomass. *Carbon* **2017**, *118*, 431–437. [CrossRef]
20. Zhang, S.; Zheng, M.; Lin, Z.; Li, N.; Liu, Y.; Zhao, B.; Pang, H.; Cao, J.; He, P.; Shi, Y. Activated carbon with ultrahigh specific surface area synthesized from natural plant material for lithium-sulfur batteries. *J. Mater. Chem. A* **2014**, *2*, 15889–15896. [CrossRef]
21. Gao, F.; Geng, C.; Xiao, N.; Qu, J.; Qiu, J. Hierarchical porous carbon sheets derived from biomass containing an activation agent and in-built template for lithium ion batteries. *Carbon* **2018**, *139*, 1085–1092. [CrossRef]
22. Niksiar, A.; Nasernejad, B. Activated carbon preparation from pistachio shell pyrolysis and gasification in a spouted bed reactor. *Biomass Bioenergy* **2017**, *106*, 43–50. [CrossRef]
23. Van, K.L.; Thi, T.T.L. Activated carbon derived from rice husk by NaOH activation and its application in supercapacitor. *Progress Nat. Sci. Mater. Int.* **2014**, *24*, 191–198. [CrossRef]
24. Kalderis, D.; Bethanis, S.; Paraskeva, P.; Diamadopoulos, E. Production of activated carbon from bagasse and rice husk by a single-stage chemical activation method at low retention times. *Bioresour. Technol.* **2008**, *99*, 6809–6816. [CrossRef] [PubMed]
25. Zhang, L.; Tu, L.-Y.; Liang, Y.; Chen, Q.; Li, Z.-S.; Li, C.-H.; Wang, Z.-H.; Li, W. Coconut-based activated carbon fibers for efficient adsorption of various organic dyes. *RSC Adv.* **2018**, *8*, 42280–42291. [CrossRef]
26. Ngernyen, Y.; Tangsathitkulchai, C.; Tangsathitkulchai, M. Porous properties of activated carbon produced from eucalyptus and Wattle wood by carbon dioxide. *Korean J. Chem. Eng.* **2006**, *23*, 1046–1054. [CrossRef]
27. Wu, F.C.; Tseng, R.L.; Juang, R.S. Preparation of highly microporous carbons from fir wood by KOH activation for adsorption of dyes and phenols from water. *Sep. Purif. Technol.* **2005**, *47*, 10–19. [CrossRef]
28. Villegas, J.P.; Valle, J.F.P.; Rodríguez, J.M.M.; García, M.G. Study of commercial wood charcoals for the preparation of carbon adsorbents. *J. Anal. Appl. Pyrolysis* **2006**, *76*, 103–108. [CrossRef]
29. Adinata, D.; Daud, W.M.W.; Aroua, M.K. Preparation and characterization of activated carbon from palm shell by chemical activation with K_2CO_3. *Bioresour. Technol.* **2007**, *98*, 145–149. [CrossRef] [PubMed]
30. Ahmad, A.L.; Loh, M.M.; Aziz, J.A. Preparation and characterization of activated carbon from oil palm wood and its evaluation on Methylene blue adsorption. *Dyes Pigm.* **2007**, *75*, 263–272. [CrossRef]
31. Jaguaribe, E.F.; Medeiros, L.L.; Barreto, M.C.S.; Araujo, L.P. The performance of activated carbons from sugarcane bagasse, babassu, and coconut shells in removing residual chlorine. *Braz. J. Chem. Eng.* **2005**, *22*, 41–47. [CrossRef]
32. Adhikari, M.P.; Adhikari, R.; Shrestha, R.G.; Rajendran, R.; Adhikari, L.; Bairi, P.; Pradhananga, R.R.; Shrestha, L.K.; Ariga, K. Nanoporous activated carbon derived from agro-waste corncob for enhanced electrochemical and sensing performance. *Bull. Chem. Soc. Jpn.* **2015**, *88*, 1108–1115. [CrossRef]
33. Shrestha, L.K.; Adhikari, L.; Shrestha, R.G.; Adhikari, M.P.; Adhikari, R.; Hill, J.P.; Pradhananga, R.R.; Ariga, K. Nanoporous carbon materials with enhanced supercapacitance performance and non-aromatic chemical sensing with C_1/C_2 alcohol discrimination. *Sci. Technol. Adv. Mater.* **2016**, *17*, 483–492. [CrossRef] [PubMed]

34. Pradhananga, R.R.; Adhikari, L.; Shrestha, R.G.; Adhikari, M.P.; Rajbhandari, R.; Ariga, K.; Shrestha, L.K. Wool carpet dye adsorption on nanoporous carbon materials derived from agro-product. *C* **2018**, *3*, 12. [CrossRef]
35. Rajbhandari, R.; Shrestha, L.K.; Prokhrel, B.P.; Pradhananga, R.R. Development of nanoporous structure in carbons by chemical activation with zinc chloride. *J. Nanosci. Nanotechnol.* **2013**, *13*, 2613–2623. [CrossRef] [PubMed]
36. Rajbhandari, R.; Shrestha, L.K.; Pradhananga, R.R. Nanoporous activated carbon derived from Lapsi (*Choerospondias axillaris*) seed stone for the removal of arsenic from water. *J. Nanosci. Nanotechnol.* **2012**, *12*, 7002–7009. [CrossRef] [PubMed]
37. Luna, M.D.G.D.; Flores, E.D.; Genuino, D.A.D.; Futalan, C.M.; Wan, M.W. Adsorption of erichrome black T (EBT) dye using activated carbon prepared from waste rice hulls- optimization, isotherm and kinetic studies. *J. Taiwan Inst. Chem. Eng.* **2013**, *44*, 646–653. [CrossRef]
38. Bakar, R.A.; Yahya, R.; Gan, S.N. Production of high purity amorphous silica from rice husk. *Procedia Chem.* **2016**, *19*, 189–195. [CrossRef]
39. Daifullah, A.A.; Girgis, B.S.; Gad, H.M. Utilization of Agro-residues (rice husk) in small wastewater treatment plants. *Mater. Lett.* **2003**, *57*, 1723–1731. [CrossRef]
40. Alvarez, J.; Lopez, G.; Amutio, M.; Bilbao, J.; Olazar, M. Physical activation of rice husk pyrolysis char for the production of high surface area activated carbons. *Ind. Eng. Chem. Res.* **2015**, *54*, 7241–7250. [CrossRef]
41. Della, V.P.; Kuhn, I.; Hotza, D. Rice husk ash as an alternate source for active silica production. *Mater. Lett.* **2002**, *57*, 818–821. [CrossRef]
42. Naskar, M.K.; Chatterjee, M. A novel process for the synthesis of cordierite ($Mg_2Al_4Si_5O_{18}$) powders from rice husk ash and other sources of silica and their comparative study. *J. Eur. Ceram. Soc.* **2004**, *24*, 3499–3508. [CrossRef]
43. Mohamed, R.M.; Khalid, I.A.M.; Barakat, M.A. Rice husk ash as a renewable source for the production of zeolite NaY and its characterization. *Arab. J. Chem.* **2015**, *8*, 48–53. [CrossRef]
44. Liou, T.H.; Wu, S.J. Characteristics of microporous/mesoporous carbons prepared from rice husk under base- and acid- treated conditions. *J. Hazard. Mater.* **2009**, *171*, 693–703. [CrossRef] [PubMed]
45. Zhang, X.; Li, G.; Hu, C. Preparation of Fe/activated carbon directly from rice husk pyrolytic carbon and its application in catalytic hydroxylation of phenol. *RSC Adv.* **2014**, *5*, 4984–4992. [CrossRef]
46. Al-Amsyar, S.M.; Adam, F.; Ng, E. Aluminium oxide-silica/carbon components from rice husk as a bi-functional heterogeneous catalyst for the one-pot sequential reaction in the conversion of glucose. *Surf. Interfaces* **2017**, *9*, 1–8. [CrossRef]
47. Liu, N.; Huo, K.; McDowell, M.T.; Zhao, J.; Cui, Y. Rice husks as a sustainable source of nanostructured silicon for high performance Li-ion battery anodes. *Sci. Rep.* **2013**, *3*, 1919. [CrossRef]
48. Wang, L.; Schnepp, Z.; Titirici, M.M. Rice husk-derived carbon anodes for lithium ion batteries. *J. Mater. Chem. A* **2013**, *1*, 5269–5273. [CrossRef]
49. Singh, P.; Bahadur, J.; Pal, K. One-step one chemical synthesis process of graphene from rice husk for energy storage applications. *Sci. Res.* **2017**, *6*, 61–71. [CrossRef]
50. Teo, E.Y.L.; Muniandy, L.; Ng, E.; Adam, F.; Mohamed, A.R.; Jose, R.; Chong, K.F. High surface area activated carbon from rice husk as a high performance supercapacitor electrode. *Electrochim. Acta* **2016**, *192*, 110–119. [CrossRef]
51. Guo, Y.P.; Yang, S.F.; Yu, K.F.; Zhao, J.Z.; Wang, Z.C.; Xu, H.D. The preparation and mechanism studies of rice husk based porous carbon. *Mater. Chem. Phys.* **2002**, *74*, 320–323. [CrossRef]
52. Masoud, M.S.; El-Saraf, V.M.; Abdel-Halim, A.M.; Ali, A.E.; Mohamed, E.A.; Hasan, H.M.I. Rice husk and activated carbon for waste water treatment for El-Mex Bay, Alexandria Cost, Egypt. *Arabian J. Chem.* **2016**, *9*, S1590–S1596. [CrossRef]
53. Rhaman, M.T.; Haque, M.; Rouf, M.A.; Siddique, M.A.B.; Islam, M.S. Preparation and characterization of activated carbon and amorphous silica from rice husk. *Bangladesh J. Sci. Ind. Res.* **2015**, *50*, 263–270. [CrossRef]
54. Kalapathy, U.; Proctor, A.; Shultz, J. A simple method for production of pure silica from rice hull ash. *Bioresour. Technol.* **2000**, *73*, 257–262. [CrossRef]
55. ASTM. *American Society of Testing Materials*; ASTM: Philadelphia, PA, USA, 1994; pp. D3173–D3175, D4607.

56. Terzyk, A.P. The influence of activated carbon surface chemical composition on the adsorption of acetaminophen (paracetamol) in vitro: Part II. TG, FTIR, and XPS analysis of carbons and the temperature dependence of adsorption kinetics at the neutral pH. *Colloids Surf.* **2001**, *177*, 23–45. [CrossRef]
57. Al-Oweini, R.; El-Rassy, H. Synthesis and characterization by FTIR spectroscopy of silica aerogels prepared using several Si(OR)4 and R″Si(OR′)3 precursors. *J. Mol. Struct.* **2009**, *919*, 140–145. [CrossRef]
58. Osica, I.; Imamura, G.; Shiba, K.; Ji, Q.; Shrestha, L.K.; Hill, J.P.; Kurzydłowski, K.J.; Yoshikawa, G.; Ariga, K. Highly Networked Capsular Silica−Porphyrin Hybrid Nanostructures as Efficient Materials for Acetone Vapor Sensing. *ACS Appl. Mater. Interfaces* **2017**, *9*, 9945–9954. [CrossRef]
59. Li, Z.Q.; Lu, C.J.; Xia, Z.P.; Zhou, Y.; Luo, Z. X-ray diffraction patterns of graphite and turbostratic carbon. *Carbon* **2007**, *45*, 1686–1695. [CrossRef]
60. Shrestha, L.K.; Shrestha, R.G.; Yamauchi, Y.; Hill, J.P.; Nishimura, T.; Miyazawa, K.; Kawai, T.; Okada, S.; Wakabayashi, K.; Ariga, K. Nanoporous carbon tubes from fullerene crystal as the π-electron carbon source. *Angew. Chem. Int. Ed.* **2015**, *54*, 951–955. [CrossRef]
61. Bairi, P.; Shrestha, R.G.; Hill, J.P.; Nishimura, T.; Ariga, K.; Shrestha, L.K. Mesoporous graphitic carbon microtubes derived from fullerene C_{70} tubes as a high performance electrode material for advanced supercapacitors. *J. Mater. Chem. A* **2016**, *4*, 13899–13906. [CrossRef]
62. Maciá-Agulló, J.A.; Moore, B.C.; Cazorla-Amorós, D.; Linares-Solano, A. Influence of carbon fibres crystallinities on their chemical activation by KOH and NaOH. *Microporous Mesoporous Mater.* **2007**, *101*, 397–405. [CrossRef]
63. Ferrari, A.C.; Robertson, J. Interpretation of Raman spectra of disordered and amorphous carbon. *Phys. Rev. B* **2000**, *61*, 14095–14107. [CrossRef]
64. Lee, J.; Kim, J.; Hyeon, T. Recent progress in the synthesis of porous carbon materials. *Adv. Mater.* **2006**, *18*, 2073–2094. [CrossRef]
65. Magana, J.R.; Kolen'ko, Y.V.; Deepak, F.L.; Solans, C.; Shrestha, R.G.; Hill, J.P.; Ariga, K.; Shrestha, L.K.; Rodriguez-Abreu, C. From chromonic self-assembly to hollow carbon nanofibers: Efficient materials in supercapacitor and vapor-sensing applications. *ACS Appl. Mater. Interfaces* **2016**, *8*, 31231–31238. [CrossRef] [PubMed]
66. Ma, T.-Y.; Liu, L.; Yuan, Z.-Y. Direct synthesis of ordered mesoporous carbons. *Chem. Soc. Rev.* **2013**, *42*, 3977–4003. [CrossRef]
67. Liou, T. Development of mesoporous structure and high adsorption capacity of biomass-based activated carbon by phosphoric acid and zinc chloride activation. *Chem. Eng. J.* **2010**, *158*, 129–142. [CrossRef]
68. Raposo, R.; Rubia, M.A.D.L. Methylene blue number as useful indicator to evaluate the adsorptive capacity of granular activated carbon in batch mode: Influence of adsorbate/adsorbent mass ratio and particle size. *J. Hazard. Mater.* **2009**, *165*, 291–299. [CrossRef]
69. Nunes, C.A.; Guerreiro, M.C. Estimation of surface area and pore volume of activated carbons by methylene blue and iodine numbers. *Quim. Nova* **2011**, *34*, 472–476. [CrossRef]
70. Li, Y.; Du, Q.; Liu, T.; Peng, X.; Wang, J.; Sun, J.; Wang, Y.; Wu, S.; Wang, Z.; Xia, Y.; et al. Comparative study of methylene blue dye adsorption onto activated carbon, graphene oxide, and carbon nanotubes. *Chem. Eng. Res. Des.* **2013**, *91*, 361–368. [CrossRef]